Engineering Structures 343 (2025) 121238

Contents lists available at ScienceDirect

Engineering Structures

journal homepage: www.elsevier.com/locate/engstruct

# Interpretation of experimental investigations on framed timber shear walls using numerical investigations of Daniels Systems

L. Kramer [a,b,*,1], M. Geiser [a,2], D. Proske [c]

[a] Bern University of Applied Sciences, Institute for Timber Construction, Solothurnstrasse 102, Biel CH-2500, Switzerland
[b] Swiss federal laboratories for material sciences and technology, Structural Engineering Research Labratory, Ueberlandstrasse 129, Dübendorf CH-8600, Switzerland
[c] Bern University of Applied Sciences, Institute for Infrastructure and Environment, Pestalozzistrasse 20, Burgdorf CH-3400, Switzerland

ARTICLE INFO

*Keywords:*
Structural engineering
Timber engineering
Framed timber shear walls
Sheathing
Eurocode 5
Reduction factor
Daniels System

ABSTRACT

Framed timber shear walls (FTSW) represent a widely used construction technique. They can be constructed with one- or two-sided sheathing. For the design, reduction factors are required as additional stresses are present in the sheathing panels which are not taken into account in the shear field model, which serves as the basis in design standards such as Eurocode 5. Based on recent experimental studies such factors have been developed empirically. However, a theoretical explanation is needed for the smaller reduction factors $k_{p,model}$ of two-sided sheathing compared to one-sided sheathing of FTSW. In this study, the theoretical Daniels System was selected and numerical investigations using this model were carried out to provide a possible explanation for the observed results. These numerical results were used to derive the expected peak force of two-side sheathed FTSW based on the experimental results of one-side sheathed FTSW. The results show that the model properties can indeed provide an explanation for the reduced reduction factors found by the experimental studies on FTSW. Thus, the reduction factor $k_{p,model}$ can be determined from one-side sheathed FTSW alone.

## 1. Introduction

Urban densification requires buildings to be higher [1]. Therefore, bracing systems gain importance and have to get stronger. For timber structures there are two possibilities to do this, one way is to use an inherently stronger system such as reinforced concrete cores or steel frames. Another way is to optimise the widely applied construction method of framed timber shear walls (FTSW), or other timber-based bracing systems. This study focuses on the issue of the optimisation of the design of FTSW (see Fig. 1 for a visual representation of the elements of a FTSW).

The perennial issue in the design of FTSW is the determination of the resistance of the sheathing. Different codes lead to vastly different calculated resistances [2–6]. Some require a reduction of the resistance due to additional stresses in the sheathing panel like DIN 1052:2008, DIN EN 1995–1-1:2008 and prEN 1995–1-1:2023–04 [2,4,6], while others don't [3–5]. The resistance side of the verification of the sheathing panel of a FTSW in prEN 1995–1-1:2023–04 [6] as shown in Eq. (1) has three terms: the design shear strength $f_{p,v,d}$, the factor accounting for buckling of the panel in shear $k_{p,v}$, and the model factor (called reduction factor from here) accounting for additional stresses in the sheathing panel $k_{p,model}$. The $k_{p,model}$ factors specified in prEN 1995-1-1:2023-04 [6] are given in Table 1.

$$\tau_d \leq k_{p,model} \quad k_{p,v} \quad f_{p,v,d} \tag{1}$$

Qualitative causes for the additional stresses are given in the note of prEN 1995–1-1:2023–04, clause 12.2.4(4) [6]:

- Uneven shear stress distribution around sheathing panels;
- Nominal forces perpendicular to the sheathing edges;
- The eccentricity between the frame axes and the axis of the sheathing for diaphragms with sheathing fixed to one side of the framing only;
- The eccentricity of the axes of framing arranged in multiple layers;
- Other simplifications in the strength model compared to reality.

*Abbreviations:* CI, Confidence Interval; CoV, Coefficient of Variation; D, Ductility of an element; $F_{max}$, Peak force; FTSW, Framed timber shear walls; GFB, Gypsum fibre board; $k_{p,\ model}$, Reduction factor; OSB, Oriented strand board; $\delta_{peak}$, Displacement at peak force; α, Number of tests, Significance leveln.

* Corresponding author at: Bern University of Applied Sciences, Institute for Timber Construction, Solothurnstrasse 102, Biel CH-2500, Switzerland.
*E-mail addresses:* lukas.kramer@bfh.ch (L. Kramer), martin.geiser@bfh.ch (M. Geiser), dirk.proske@bfh.ch (D. Proske).
[1] https://orcid.org/0009-0002-0539-3512
[2] https://orcid.org/0000-0002-1630-9120

https://doi.org/10.1016/j.engstruct.2025.121238
Received 4 February 2025; Received in revised form 22 July 2025; Accepted 22 August 2025
Available online 4 September 2025

Regarding other simplifications in the strength model compared to reality, the connection between framing members is mentioned specifically by Manser et al. [7]. The shear field theory assumes pinned connections of the framing members while in reality the connection has a rotational as well as longitudinal and transversal stiffness which deviates from the shear field model assumption.

Quantitative evaluations of the individual causes are still open.

Most publications on FTSW focus explicitly or implicitly on the investigation of dissipative failure [8–18]. The sheathing of these FTSW was intentionally oversized to ensure plasticisation of the sheathing to framing connection. While the investigation of dissipative failure is important research, no information on the resistance of the sheathing can be extracted. In recent experimental investigations [7,19] on the resistance of the sheathing, sheathing failure was intentionally induced by over-designing of the other FTSW components relative to the sheathing. The results obtained showed significant deviation from expected outcomes based on current standards [2,4,6]. According to the aforementioned sources, the peak force at sheathing failure of two-side sheathed FTSW was expected to be more than twice the force of one-side sheathed FTSW [2,4,6]. However, this was not confirmed by experiments [7,19]. The authors are not aware of any background documents for the distinction of one-sided and two-sided sheathing and the absolute value of the reduction factor $k_{p,model}$ in [2,4,6]. Consequently, there is currently no explanation for this code contradiction, i.e. the experimental determination of the load carrying capacity of the FTSW shows a larger reduction for two-side sheathed walls (smaller reduction factor $k_{p,model}$) compared to ones-side sheathed walls, which cannot be explained.

Therefore, the new findings are not taken into account in the development of prEN1995-1-1:2023.

A possible model to investigate the load bearing behaviour of parallel systems was developed by Daniels, 1945 [20] and is therefore called the Daniels System, shown in Fig. 2. Such a Daniels System consists of up to n elements and has perfect load sharing with infinite stiffness (later called load sharing) according to [21]. There are many investigations on Daniels Systems for time invariant investigations [20–23] as well as for time variant investigations [24–26]. All these investigations have in common, that the reliability index of the Daniels System is either the result of the investigation or the target for an optimisation.

As none of the aforementioned publications on Daniels Systems report peak forces for the investigated systems a direct application of the results for the interpretation of experimental investigations is not possible.

The paper is structured as follows: The first part summarises the experimental investigations on which this work is based. The second part describes the necessary numerical investigations on Daniels Systems. This includes the evaluation of the normalised system force for a different number of elements and different force-displacement curve characteristics. The third part compares the expected peak force per sheathing panel with the experimentally determined peak force. In addition, recommendations are made for code implementations for the sheathing resistance reduction due to other factors $k_{p,model}$ in the second generation of the Eurocode 5.

**Table 1**
Values of model factor $k_{p,model}$ as defined in prEN 1995-1-1:2023-04 [6].

| Product | Sheathing on one side | Sheathing on both sides |
|---|---|---|
| Wood-based sheathing, gypsum fibreboard | 0.5 | 0.67 |

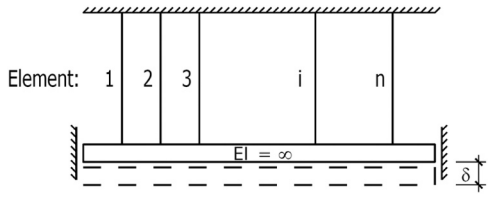


**Fig. 2.** Symbolic view of a Daniels System.

## 2. Description of the experimental investigations

This section summarises the two experimental studies [7,19] on which this work is based. For a more detailed overview of these investigations, the reader is referred to the original documents.

In both studies, the FTSW were designed to induce failure in the sheathing. The walls were fully anchored (e.g. a hold-down prevents the vertical stud on the side the force is applied to the wall from uplift) to the test frame. A reduction factor $k_{p,model} = 1.0$ was used in the design as a starting point for the investigation. The static-monotonic loading protocol of the ISO 21581:2010–06 [27] was applied. Tilting of the wall was avoided at the top of the wall.

### 2.1. Tests on OSB/3 sheathed FTSW

In Manser et al. [7] the sheathing capacity of the oriented strand board (OSB) was investigated. Nine series of FTSW triplicates were tested, given a total of 27 specimens. The three quadratic one-side sheathed FTSW with sheathing thickness 12 mm (Q-12-S) and the

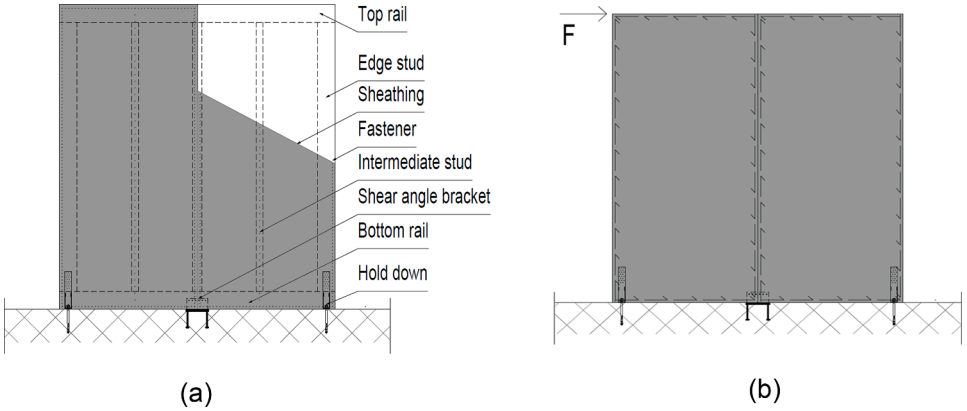


**Fig. 1.** (a) Schematic drawing of a FTSW with labelling of the elements, (b) Shear field which results in the framing which serves as the basis for the model in design standards such as prEN 1995–1-1:2023–04 [6].

FTSW with the same specification but two-sided sheathing (Q-12-S-2S) are used in this investigation. The main specifications and the peak force $F_{max}$ are compiled in Table 2.

The test setup is shown in Fig. 3. The vertical displacement of the horizontal edge stud was measured with linear variable differential transformers (LVDTs). The fastener and sheathing arrangement on the timber frame is shown Fig. 4 and the specific values are noted in Table 2.

Shear strength tests were carried out on panels from the same batch as the sheathing of the FTSW. The shear strength tests of the OSB/3 panels were carried out according to EN 789:2005–01 [28]. For both strand orientations, 6 specimens were tested at each panel thickness of interest. Based on all shear tests, Manser et al. [7] defined a lower bound of the coefficient of variation (CoV) of 6 %. An exemplary force-displacement curve is shown in Fig. 5.

Based on the experimental tests summarized in this section, a $k_{p,model}$ value of 0.6 for one and two-side sheathed FTSW with OSB/3 sheathings was suggested in [7].

### 2.2. Tests on GFB sheathed FTSW

In Kramer et al. [19] the sheathing capacity of gypsum fibre board (GFB) was investigated. A total of 16 FTSW of eight types were tested. Two types of FTSW were tested, allowing a comparison between one-sided and two-sided sheathing. Two samples were tested for each configuration. The first series (2-WSX1-r15-a2x30) was tested upright and the second series (3-WSX1-r15-a2x50) was tested horizontally as shown in Fig. 6 and as the FTSW in Section 2.1. The only other difference of the FTSW was the fastener spacing. The first series had a fastener spacing of 30 mm whilst the second series had a fastener spacing of 50 mm, further information on the fastener and sheathing arrangement is given in Table 3. The vertical displacement of the vertical studs was measured with LVDTs.

The shear strength capacity of GFB was provided by the manufacturer of the panels. A total of ten specimens were tested for each production direction. The CoV was determined to be 4.6 % as the mean of the CoV of both production directions, based on unpublished test series by another test institute. The characteristics of a typical force-displacement curve of GFB are shown in a normalised graph in Fig. 7.

For FTSW with GFB sheathing a reduction factor $k_{p,model}$ of 0.33 for one and two-side sheathed FTSW was suggested in [19].

### 2.3. System classification

The tested FTSWs were designed such that failure occurs in the sheathing. Consequently, the timber frame (studs and rails) and the sheathing to framing connection was strongly over-designed with respect to the resistance of the sheathing panels. Further details to support this statement can be found in [7,19]. Consequently, the deformation of the FTSW, as outlined in Sections 2.1 and 2.2 is predominantly concentrated in the sheathing. The top and bottom rails undergo only very small and therefore negligible deformations. The deformations in the fasteners are negligible due to the high number of fasteners. Thus, the sheathing panel of the FTSW corresponds to the elements in the Daniels System and the studs, rails, and fasteners of the FTSW correspond to the load sharing in the Daniels System, as illustrated in Fig. 8. In Fig. 8, the FTSW has two-sided sheathing and thus, the Daniels System has two elements as each sheathing panel is represented by one element. It is acknowledged that, as with every model the Daniels System includes some simplifications, such as EI = ∞ for the load sharing. Nevertheless, it is considered beneficial to provide a description of the observed phenomena. Consequently, the parallel load-bearing capacity of the sheathing of a FTSW is classified as a Daniels System.

**Table 2**
Properties of the tested FTSW with OSB/3 sheathing.

| | | | Q-12-S | Q-12-S-2S |
|---|---|---|---|---|
| Sheathing | Thickness | [mm] | 12 | 12 |
| | One- or two-sided | [nr] | 1 | 2 |
| Fasteners | Type | | Staple 1.53 × 50 | Staple 1.53 × 50 |
| | Rows at sheathing edge | [nr] | 8 | 8 |
| | Rows on interm. studs | [nr] | 2 | 2 |
| Distances | $d_1$ | [mm] | 20 | 20 |
| | $d_2$ | [mm] | 20 | 20 |
| | $d_3$ | [mm] | 25 | 25 |
| | $d_4$ | [mm] | 25 | 25 |
| | $d_5$ | [mm] | 20 | 20 |
| | $d_6$ | [mm] | 20 | 20 |
| | $a_v$ | [mm] | 23 | 23 |

## 3. Numerical investigations

This section presents the numerical investigations conducted on Daniels Systems, exploring the influence of different force-displacement characteristics. The investigation is material independent and is applicable to all systems that meet the definition of a Daniels System and the characteristics of the systems described in Section 3.1. Thus, more than two elements, as needed for the application to FTSW as shown in Fig. 8, are investigated for the numerical investigations to be applicable beyond the FTSW. The most important properties of a Daniels System are [20]:

- The action is quasi-static
- All elements have the same deflection (due to EI = ∞ of the load sharing)

### 3.1. Methods

For the investigation of the Daniels System characteristics, crude Monte Carlo simulations of the material properties were made.

#### 3.1.1. Ductility and number of elements per system

The ductility of materials, elements and connections is an important characteristic that has been the focus of extensive research [30–39]. Thus, the influence of multiple ductility levels on the system characteristics is studied. The ductility measure utilised in this study draws inspiration from the approach employed by Gollwitzer & Rackwitz [21]. A minor adjustment has been made to ensure a dimensionless measure. The new measure is defined in Eq. (2), resulting in a ductility of zero for a linear elastic brittle system. Conversely, for a bilinear system that sustains the maximum force up to twice the yield displacement, the resulting ductility is 1. The range of ductility levels investigated is described in the Section 3.1.2. In Eq. (2), d is the ductility, $\delta_{peak}$ is the lowest displacement at maximum force, $F_{max}$ is the maximum force and $F(\delta)$ is the force at a given displacement $\delta$.

$$d = \frac{\int_0^{2\delta_{peak}} F(\delta)d\delta - \frac{(F_{max}\cdot\delta_{peak})}{2}}{(F_{max}\cdot\delta_{peak})} \quad (2)$$

The numerical investigations were conducted for systems comprising 2, 3, 5 and 10 elements, respectively. As reference a single element was used.

#### 3.1.2. Force – displacement curves of the elements of the system

The investigation focuses on two distinct groups of force-displacement curves. The first group is designated as bilinear, while the second group is designated curved due to the absence of a distinct linear elastic behaviour which leads to a total of four different force-displacement curve types. The displacement at peak force $\delta_{peak}$ is

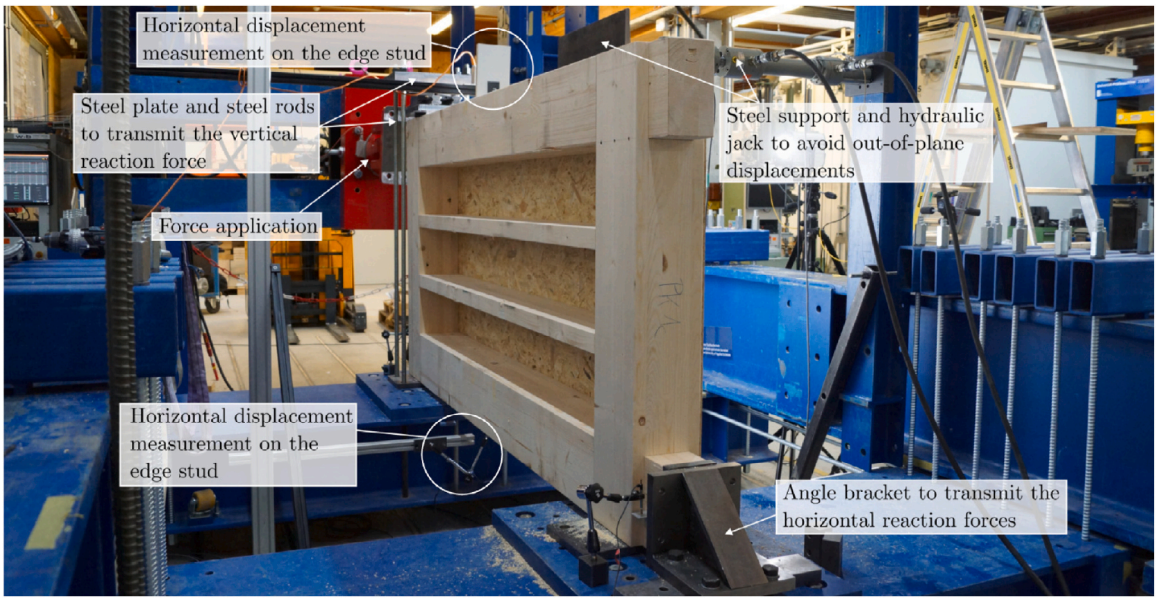


**Fig. 3.** Test setup of the OSB/3 sheathed FTSW [7].

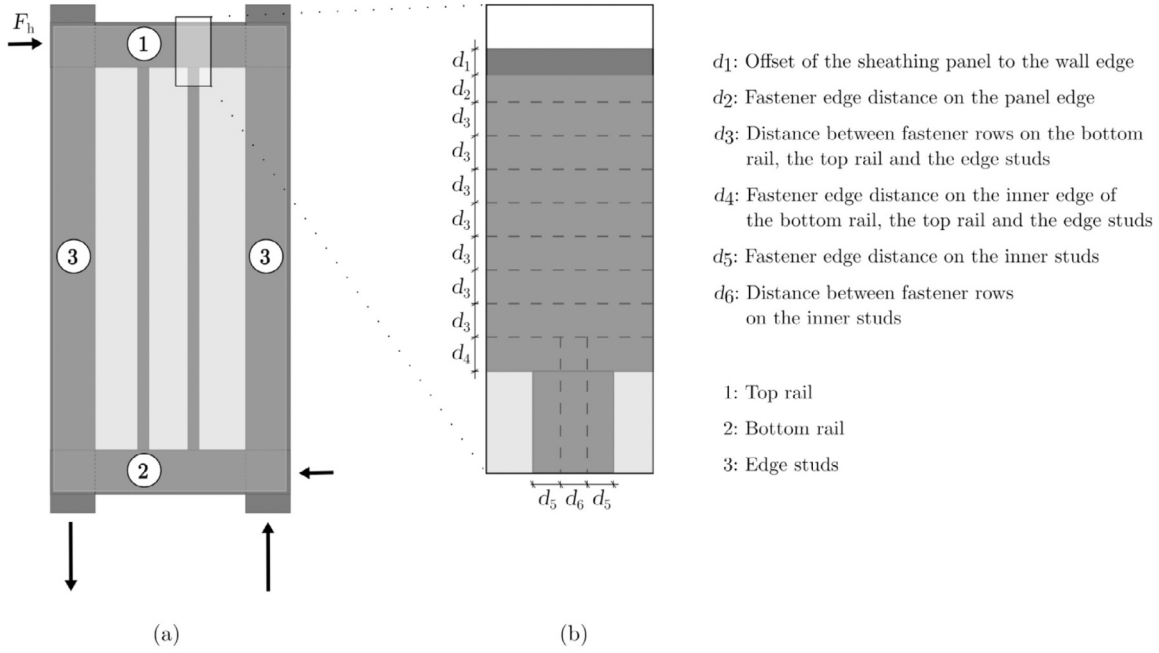


**Fig. 4.** Fastener arrangement of the OSB/3 sheathed FTSW tests [7].

equal for all force-displacement curves, under the condition that all parameters are equal to the mean.

Two types of bilinear curves are investigated. The first type of bilinear curve is characterised by holding a constant force over the displacement between $\delta_{peak}$ and $2\delta_{peak}$. The constant force is dependent on the targeted ductility as shown in Fig. 9(a). The second type of bilinear curve is characterized by holding the maximal force over a different displacement. The length the maximal force is held is dependent on the targeted ductility as illustrated in Fig. 9(b). Both types are investigated for ductilities between 0 and 1 in an interval of 0.25.

This study investigates two types of curved force-displacement curves. The basis of both types is the model proposed by Doland and Foschi [40]. The first type of curve is characterised by a model with all variables equal to the mean, resulting in a ductility of 0.1 within the range between 0 and $\delta_{peak}$. The targeted ductility is achieved by adjusting the stiffness after $\delta_{peak}$ for each realisation of the model individually. The range of ductilities investigated is from 0.25 to 1, with an increment of 0.25, as illustrated in Fig. 10 (a). The subsequent model, characterised by strongly curved force displacement curves, exhibits a ductility of 0.25, with all variables equal the mean within the range from 0 to $\delta_{peak}$. The investigation of ductilites between 0.25 and 1.25 is conducted within an interval of 0.25, as illustrated in Fig. 10 (b).

### 3.1.3. Sample generation

The target value of the numerical analysis is the reliability and the mean peak force. The assumption is made that all random parameters follow a Log-normal distribution, with a CoV of 10 %. This is consistent with the range of most material properties as listed in the JCSS [41–44].

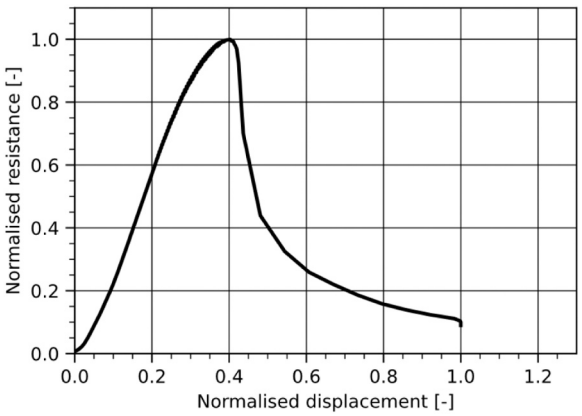


**Fig. 5.** Normalised force-displacement curve of OSB/3 shear test. Data from Manser, dissertation in preparation [29], further information will be supplied on request.

Furthermore, negative samples are avoided in the Monte Carlo simulation by using the lognormal distribution. In addition, the Log-normal distribution follows the central limit theorem in its multiplicative form. It is further postulated that no correlation exists between the parameters of an element, nor between the same parameter of different elements. This assumption has been adopted in numerous reliability investigations because the statistical proof of correlations requires large sample sizes, which are often not realisable from an experimental point of view [45–47].

In order to analyse the reliability, numerical investigations are made using Monte Carlo simulations. The number of samples is chosen so that the findings have an acceptable margin of error with a reliability index of $\beta = 4.2$. This corresponds to a probability of failure ($p_f$) of around $10^{-5}$. According to Melchers and Beck [48], between $3 \bullet 10^5$ and $2 \bullet 10^6$ samples are required. Huang et al. [49] state that $10^7$ samples are necessary. In this study, $5 \bullet 10^6$ systems of each variant have been calculated. The samples were generated with the Python package SciPy [50].

### 3.1.4. From element to system properties

Sections 3.1.2 and 3.1.3 defined the properties of a single element. As these investigations are concerned with Daniels System properties, this section will show how the system properties were derived from the element properties. As stated in Chapter 3, each element in a Daniels System experiences the same deflection at a given time. Therefore, the force of each element in the system is summed up piecewise at the same deflection as defined in Eq. (3). This calculation is done in steps of 0.01. The resulting system force-displacement curve is piecewise linear. The system property of interest is the peak force.

$$F_{sys}(\delta) = \sum_{i=1}^{n_{elem}} F_i(\delta) \tag{3}$$

With $\delta$ as displacement, $n_{\text{elem}}$ as the total number of elements of the Daniels System, $F_i(\delta)$ is the force of the $i^{th}$ element at the displacement $\delta$ and $F_{sys}(\delta)$ is the force of total force of the Daniels System at the displacement $\delta$.

### 3.1.5. Evaluation

Based on the calculated system peak force the reliability index can be determined. As there is no predefined action applied, the single element

**Table 3**
Properties of the tested FTSW with GFB sheathing.

| | | | 2-WSX1-r15-a2x30 | 3-WSX1-r15-a2x50 |
|---|---|---|---|---|
| Sheathing | Thickness | [mm] | 18 | 18 |
| Fasteners | Type | | Staple 1.53 × 50 | Staple 1.53 × 50 |
| | Rows at sheathing edge | [nr] | 2 | 2 |
| | Rows on interm. studs | [nr] | 1 | 1 |
| Distances | $d_1$ | [mm] | 20 | 20 |
| | $d_2$ | [mm] | 15 | 15 |
| | $d_3$ | [mm] | 15 | 15 |
| | $d_4$ | [mm] | 30 | 30 |
| | $d_5$ | [mm] | 40 | 40 |
| | $a_v$ | [mm] | 30 | 50 |

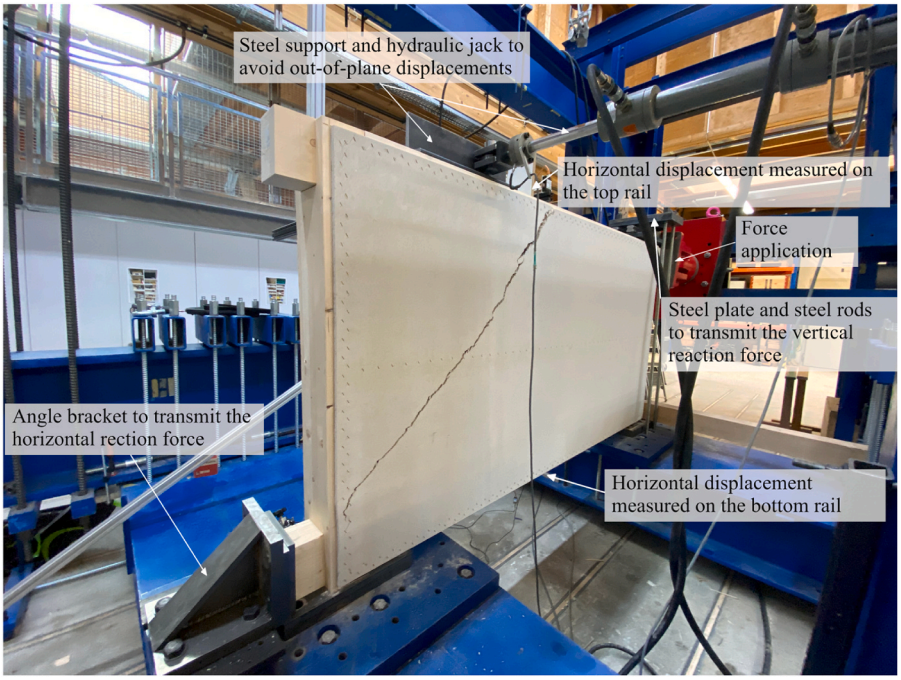


**Fig. 6.** Test setup of the GFB sheathed FTSW [19].

**Table 4**
A compendium of test specimen description and the corresponding peak force of the tested framed shear walls with OSB/3 and GFB sheathing.

| Type | Nr | $l$ x $h$ [mm] | Sheathing material | $F_{max}$ [kN] | $k_{p,model}$ [-] |
|---|---|---|---|---|---|
| One-sided | 1 | 1250 × 1250 | OSB/3 | 98 | 0.76 |
| Q−12-S | 2 | | 12 mm | 101 | |
| | 3 | | | 100 | |
| Two-sided | 1 | | | 185 | 0.69 |
| Q−12-S−2S | 2 | | | 185 | |
| | 3 | | | 179 | |
| Type 2 | 1 | 1250 × 2500 | GFB | 60.7 | 0.48 |
| 2-WS11-r15-a2x30 | 2 | | 18 mm | 61.4 | |
| One-sided | | | | | |
| Type 2 | 1 | | | 112 | 0.44 |
| 2-WS21-r15-a2x30 | 2 | | | 113 | |
| Two-sided | | | | | |
| Type 3 | 1 | 2500 × 1250 | | 233 | 0.53 |
| 3-WS11-r15-a2x50 | 2 | | | 235 | |
| One-sided | | | | | |
| Type 3 | 1 | | | 135 | 0.47 |
| 3-WS21-r15-a2x50 | 2 | | | 126 | |
| Two-sided | | | | | |

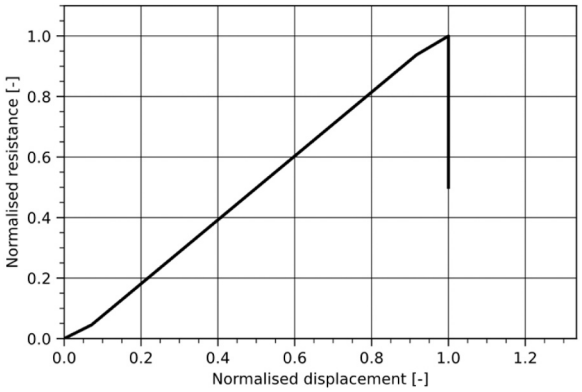


**Fig. 7.** Normalised and idealised force-displacement curve of GFB shear test.

Daniels System peak force corresponding to a target reliability index of $\beta = 2$ is computed for the Daniels System for different types of force-displacement curves in order to determine the action. The action for multi-element systems is then determined by multiplying the action force for one element by the number of elements. For the calculation of the $p_f$ on crude Monte Carlo simulations and the subsequent calculation of the reliability index the reader is referred to [48].

The second important result is the mean value of normalised peak force. Therefore, the mean of the peak system force is calculated. This average is divided by the number of elements in the system. The normalisation is based on the calculated mean system force for the system with only one element.

### 3.2. Results and discussion

The results are show separately for each type of force-displacement curve.

#### 3.2.1. Bilinear with dropping force

For all force-displacement curves characterised by a linear elastic force increasing and a drop after the maximum force, the reliability index is monotonically increasing with the number of elements. This is combined with a decreasing normalised mean peak force for all the systems studied with the number of elements. For a two-element system, the normalised mean resistance decreases between 5 % and 6 %. The only exception is a ductility of d = 1.0 for which the normalised mean peak force of the system is independent of the number of elements. This is shown in Fig. 11 (b).

Combining Figs. 3 and 6 of Gollwitzer & Rackwitz [21], these results seem plausible.

#### 3.2.2. Bilinear with yielding

The results for ductility equal to 0 and 1 are the same as in Section 3.2.1. For a ductility of 0.25, there is only a small reduction in the normalised system peak force for several elements. With a ductility of more than 0.25, there is no reduction in the normalised system force for several elements. In all cases, there is no reduction in the reliability index.

As in Fig. 11, Fig. 12 shows that ductility as defined by Eq. (2) is not a good predictor of the reliability index and the normalised Daniels System resistance. In light of Fig. 11 and Fig. 12, the chosen definition of ductility does not distinguish consistently the reliability index. The results indicate that holding the peak force over a certain displacement is a better predictor of both the reliability index and the normalised system peak force.

#### 3.2.3. Slightly curved

The reliability index does not decrease for all ductility levels of slightly curved force-displacement curves. However, the normalised system force decreases in all cases.

As can be seen by comparing Fig. 13 with Fig. 10 (a), the slightly curved force displacement curves do not hold the maximum force.

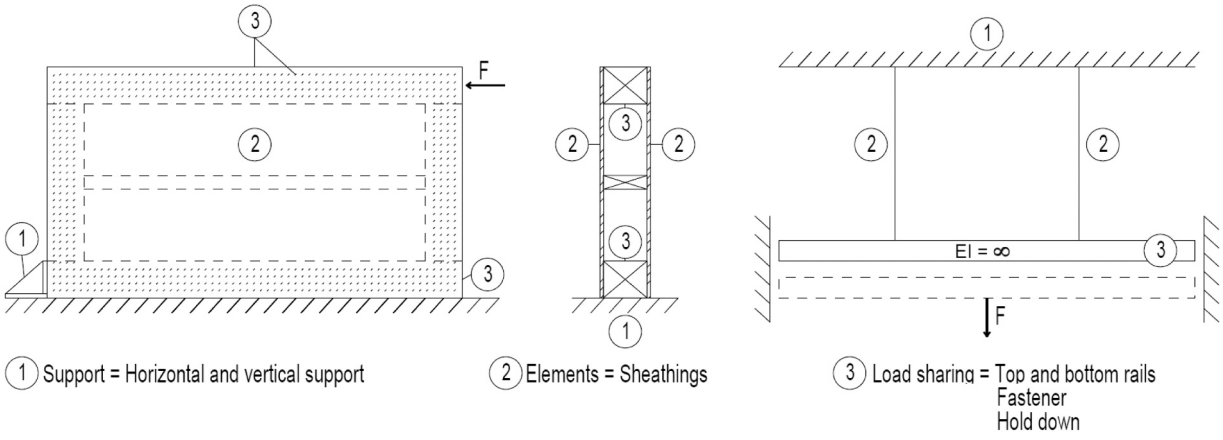


**Fig. 8.** Correspondence of the FTSW elements in the Daniels System.

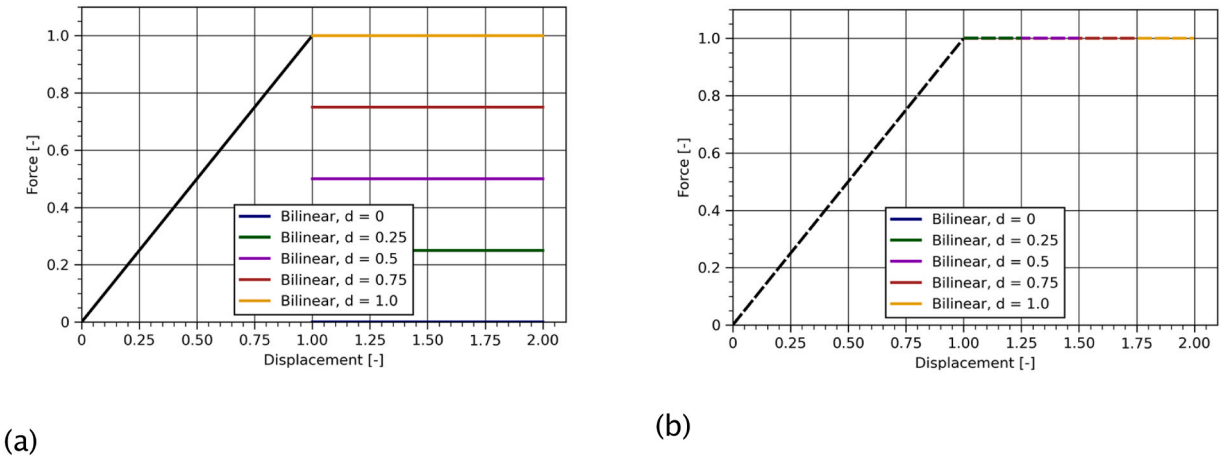


**Fig. 9.** Bilinear force - displacement curves (a) with a reduction in force after peak force (b) with a changing ultimate displacement.

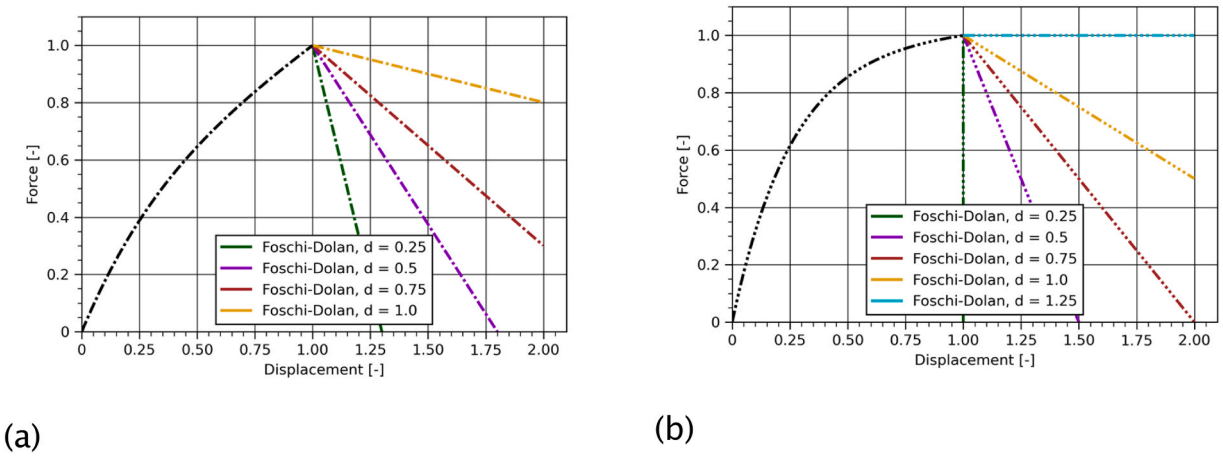


**Fig. 10.** Curved force - displacement curves (a) slightly curved (b) strong curvature.

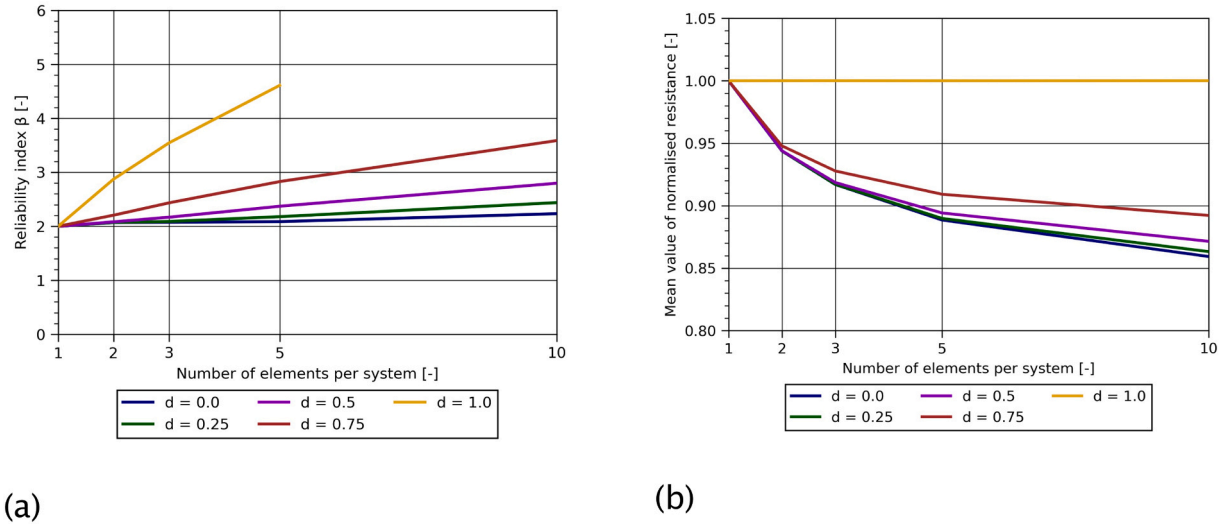


**Fig. 11.** Results of the Daniels Systems with bilinear falling force for a different number of elements (a) reliability index (b) mean value of the normalised resistance.

Knowing this, it follows that holding the maximum force over a certain displacement is an important predictor of the reliability index and the normalised system peak force.

### 3.2.4. *Heavily curved*

The reliability index for all levels of ductility for strongly curved force-displacement curves is almost the same. The calculated reliability index was found to be close to 5. However, this value should only be

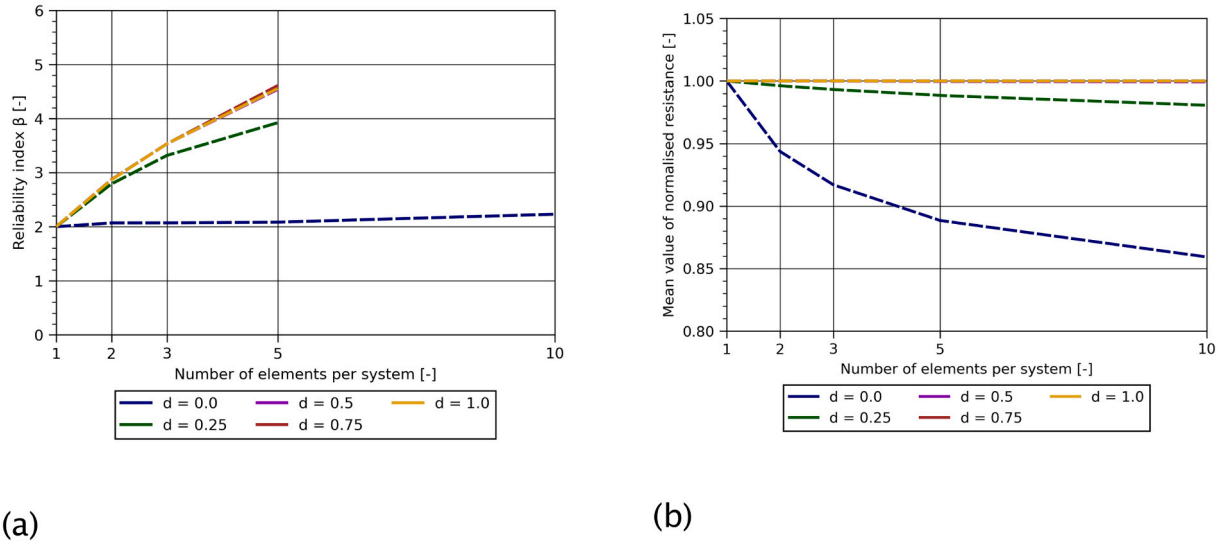


**Fig. 12.** Results of the Daniels Systems with bilinear yielding for a different number of elements (a) reliability index (b) mean value of the normalised resistance.

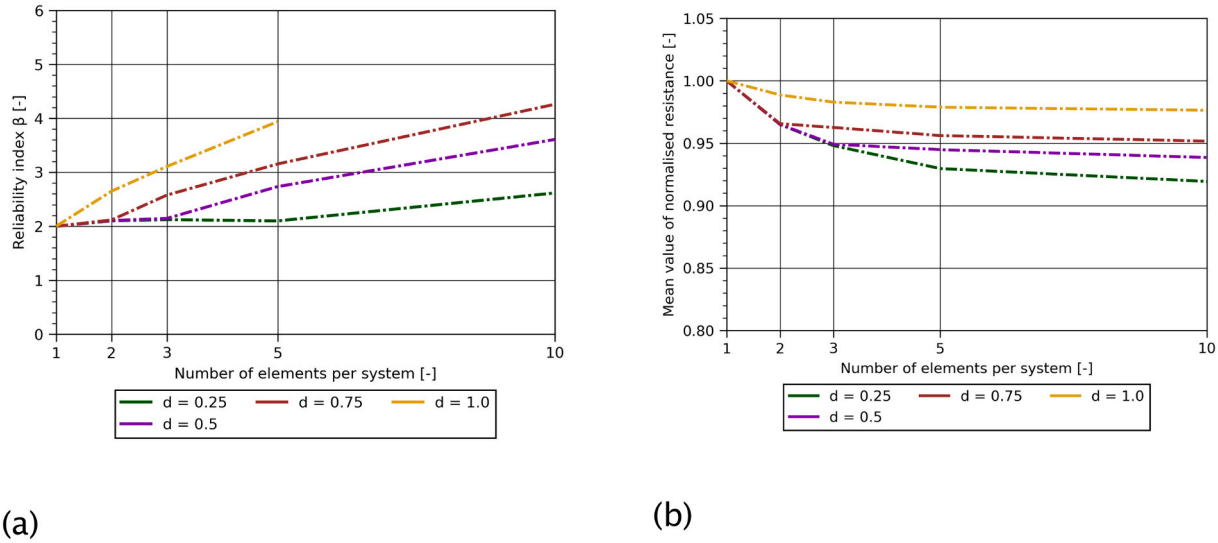


**Fig. 13.** Results of the Daniels Systems with slightly curved force-displacement curve for a different number of elements (a) reliability index (b) mean value of the normalised resistance.

taken as an order of magnitude, as it is outside the range for which the results have an acceptable margin of error according to Section 3.1.3. Except for a ductility of 1.25, the normalised system force decreases. However, the decrease is small and it is hardly possible to distinguish between the different ductility levels.

As can be seen in Fig. 14, the heavily curved force displacement curves hold the maximum force. Apart from the ductility being equal to 1.25, there is no difference between the force-displacement curves with different ductilities. This is another indication, that holding a force close to the maximum force is a better predictor of both the system reliability index and the normalised system peak force than ductility as defined in Eq. (2).

## 4. Interpretation of experimental investigations

Chapter 2 described the experimental data which formed the basis for the presented analysis. It was also shown, that the two-sided sheathing of a FTSW can be interpreted as a Daniels System. In chapter 3 the change in normalised mean system force for a different number of elements and different force-displacement curves was investigated. Therefore, in this chapter the force-displacement curve of OSB and GFB shear tests is categorised. In addition, the experimental results will be interpreted in the light of the Daniels System investigations.

### *4.1. Categorization of the force-displacement curve of the sheathing panels*

The force-displacement curve in Fig. 5 has no curvature like the models in Fig. 10. This suggests that one of the bilinear models is suitable. After reaching the maximum force, the curve is characterised by a rapid drop in force to approximately 25 % of the maximum force. Therefore, the bilinear model with a drop after reaching the maximum force, as seen in Fig. 9(a), is the closest model.

For this investigation, a higher ductility is conservative as less of the difference between one-sided and two-sided sheathing can be explained by the system effect. Therefore, the evaluated ductility according to Eq. (2) of the force-displacement in Fig. 5 of 0.39 is rounded up to 0.5.

No experimental force-displacement curve of shear tests on GFB can

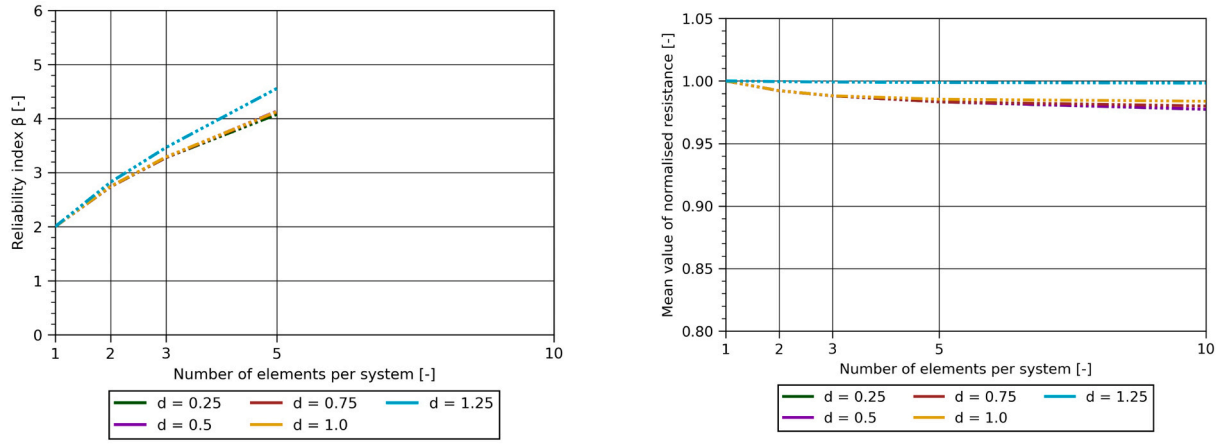


**Fig. 14.** Results of the Daniels Systems with heavily curved force-displacement curve for a different number of elements (a) reliability index (b) mean value of the normalised resistance.

be shown here. The characteristics of the force-displacement curve in Fig. 7 are almost linear with no load bearing after reaching the peak force is reached. So, they have almost no ductility and the same ductility is assumed for the GFB sheathing as for the OSB/3 sheathing. This is conservative, as the curve has less ductility than the OSB/3 curve.

### 4.2. Consideration of the system effect on the maximal force

The ductility of the OSB/3 panels has been determined to be 0.5, see Section 4.1. In contrast to the OSB/3 panels for the GFB, only general characteristics of the force-displacements curves is available. This limits evaluation of the ductility. However, it is safe to say that the ductility is lower than for the OSB/3 sheathing. Based on Fig. 11 (b) and the ductility of d = 0.5 the normalised mean force of a two-element system is 6 % smaller than the normalised force of a single element. Therefore, the expected force for two-sided sheathing is twice the mean force for the one-sided sheathing multiplied by 0.94. The expected forces are given in Table 5.

In order to decide whether the experimentally determined reduced resistance per sheathing can be explained by the system properties the confidence interval (CI) of the experimentally determined force is determined. Even tough, the sheathing resistance and the FTSW resistance were both log-normally distributed, the underlying distribution of the mean is assumed to be normally distributed. Therefore, due to the small number of shear walls tested, the students T distribution is used to construct the CI as shown in Eq. (4). In Eq. (4) $\bar{y}$ denotes the mean value of the resistance, $t_{1-\frac{\alpha}{2},n-1}$ is the value of the t-distribution for a significance level of $1-\frac{\alpha}{2}$ and a sample size $n$, the standard deviation of the resistance is denoted by $\sigma$. According to EN 1990:2002 [51], the confidence interval for individual properties should have a significance level of 75 %. Due to the small number of FTSW tested per type, the CoV from the FTSW test would not be reliable. Thus, the CoV of OSB is taken from Manser et al. [7] as 6 %, since a smaller value is a stricter condition. The sample size $n$ is equal to three as three FTSW per variant were tested from Manser et al. [7]. For the GFB sheathed FTSW, two wall types are compared, see Table 4. The CoV of GFB is given by the manufacturer to be 4.6 %. The degree of freedom is equal to two as two FTSW per variant were tested in Kramer et al. [19]. The boundaries of the CI were noted in Table 5.

$$CI = \bar{y} \pm \frac{t_{1-\frac{\alpha}{2},n-1}\sigma}{\sqrt{n}} \tag{4}$$

For all shear walls investigated, the expected force taking into account the system characteristics is within the CI. It follows that the explanation of the reduced resistance by the system properties is not refuted. However, the results show a significant statistical skewness. Statistical skewness is often an indicator of some filtering processes [52,53], which can be further investigated in the future.

**Table 5**
Confidence intervals for two-side sheathed FTSW and the expected force based on one-side sheathed FTSW considering the system characteristics.

| | Lower boundary of the CI [kN] | Upper boundary of the CI [kN] | Expected force [kN] |
|---|---|---|---|
| OSB | 174 | 192 | 187 |
| GFB Type 2 | 107 | 118 | 115 |
| Type 3 | 222 | 246 | 245 |

## 5. Conclusions

The focus of this paper was on the comparison of one-side sheathed and two-side sheathed FTSW. The present investigation did not calculate absolute values of $k_{p,model}$ as this was done in the previous studies [7,19] but investigated the reliability and mean normalised forces using the theoretical Daniels System for sheathed FTSW. The expected peak force of a two-side sheathed FTSW based on the experimental results of one-sided FTSW and on the consideration of the system characteristics in terms of a reduced contribution of one sheathing side as inferred from the Daniels System simulations, is within the CI of the peak force of the two-side sheathed FTSW. Although the mean resistance of a one-side sheathed FTSW is higher than the contribution of one-side of a two-side sheathed FTSW, the overall reliability remains the same as shown in Fig. 11 (a). Therefore, the system characteristics described as parallel load bearing of the sheathing explain the reduction in measured peak force as contribution per sheathing found by the presented experimental investigations [7,19]. The conclusion is that one and two-sided sheathing should have the same $k_{p,model}$ factor.

The result of this investigation contradicts the current codes which assume a reduced peak force for one-side sheathed FTSW compared to the contribution of one-side of a two-side sheathed FTSW. It is therefore

concluded that the different reduction factors $k_{p,model}$ in prEN1995–1-1:2024 [6] for one- and two-sided sheathing are not supported by the existing experimental investigations [7,19] or by the theoretical interpretation as demonstrated in this paper. The explanation for the reduced contribution of one sheathing in two-side sheathed FTSW due to the parallel load bearing of this investigation supports the findings of the experimental investigations [7,19]. Thus, further legitimating the findings of the two experimental studies and the proposal to have the same $k_{p,model}$ value (0.6 for OSB/3 sheathing and 0.33 for GFB sheathing) for one and two-side sheathed FTSW.

For sheathing materials not covered by prEN1995–1-1:2023, it is recommended that the $k_{p,model}$ factor should be determined on the basis of experimental investigations on one-sided sheathing if the parallel load bearing explains possible differences as shown in this paper.

As shown in Section 3.2, ductility as defined by Eq. (2) has potential for improvement as predictor of system performance. At present, maintaining a force close to the maximum force appears to be a more promising predictor. Further investigations of other definitions of the ductility shall be undertaken in the future. These definitions may be better predictors of system reliability.

## CRediT authorship contribution statement

**Lukas Kramer:** Conceptualization, Methodology, Software, Formal analysis, Writing – original draft, Writing – review & editing. **Martin Geiser:** Conceptualization, Writing – review & editing, Project administration, Funding acquisition. **Dirk Proske:** Methodology, Validation, Writing – review & editing.

## Declaration of Generative AI and AI-assisted technologies in the writing process

During the preparation of this work the authors used Deepl Write in order to improve the readability and language of the manuscript. After using this tool/service, the authors reviewed and edited the content as needed and take full responsibility for the content of the published article.

## Declaration of Competing Interest

The authors declare that they have no known competing financial interests or personal relationships that could have appeared to influence the work reported in this paper.

## Acknowledgements

This work was supported by the Swiss Federal Office for the Environment FOEN within the framework of the initiative Aktionsplan Holz 2021 – 2026, Holzbau Schweiz and Swiss Timber Engineers.

The authors would like to thank the reviewers for their critical examination and constructive feedback, which has greatly improved the quality of this manuscript.

## Data availability

Data will be made available on request.

## References

[1] Fatone S, Conticelli E, Tondelli S. Environmental sustainability and urban densification. WIT Trans Ecol Environ V 2012;155. https://doi.org/10.2495/SC120191.
[2] German Institute for Standardization DIN (2008) DIN 1052: Design of timber structures. General rules and rules for buildings.
[3] European Committee for Standardization CEN (2008) EN 1995-1-1/A1: Eurocode 5: Design of timber structures - Part 1-1: General - Common rules and rules for buildings.
[4] German Institute for Standardization DIN (2013) DIN EN 1995-1-1/NA:2013-08: Nationaler Anhang - National festgelegte Parameter - Eurocode 5: Bemessung und Konstruktion von Holzbauten – Teil 1-1: Allgemeines - Allgemeine Regeln und Regeln für den Hochbauhttps://dx.doi.org/10.31030/2025142.
[5] Swiss Association for Standardization SNV (2021) SIA 265:2021 Holzbau.
[6] European Committee for Standardization CEN (2023) prEN 1995-1-1_FOR ENQ (working draft to CIB).
[7] Manser N, Steiger R, Geiser M, Otti M, Frangi A. Shear resistance of oriented strand board panel sheathings in timber-framed shear walls. Eng Struct 2024. https://doi.org/10.1016/j.engstruct.2024.118461.
[8] Peric L., 2019, Light Frame Timber Walls in Regions of Low to Moderate Seismicity, Dissertation, ETH Zürich, https://doi.org/10.3929/ethz-b-000344004.
[9] Marzaleh AS, Nerbano S, Croce AS, Steiger R. OSB sheathed light-frame timber shear walls with strong anchorage subjected to vertical load, bending moment, and monotonic lateral load. Eng Struct 2018;173:787–99. https://doi.org/10.1016/j.engstruct.2018.05.044.
[10] Marzaleh AS, Steiger R. Experimental investigation of OSB sheathed timber frame shear walls with strong anchorage subjected to cyclic lateral loading. Eng Struct 2021;226:787–99. https://doi.org/10.1016/j.engstruct.2020.111328.
[11] Kessel M, Anheier D, Sieder M. Zur Einschätzung der Duktilität von holztafeln (I) Bautechnik 2018;95(11):801–10. https://doi.org/10.1002/bate.201800048.
[12] Hall C., Methoden zur elastischen und plastischen Modellierung von scheibenartig beanspruchten Holztafeln, Technische Universität Carlo-Wilhelmina zu Braunschweig, Braunschweig, 2012, Online available: ⟨https://nbn-resolving.org/urn:nbn:de:gbv:084-12121711087⟩.
[13] Salenikovich A.J., Dolan J.D., The racking performance of shear walls with various aspect ratios. Part 1. Monotonic tests of fully anchored walls, Forest Prod J 53(10) p. 65-73.
[14] Salenikovich AJ, Dolan JD. The racking performance of shear walls with various aspect ratios. Part 2. Cyclic tests of fully anchored walls. Prod J 1990;53(11): 37–45.
[15] Källsner B, Girhammar UA. Analysis of fully anchored light-frame timber shear walls – elastic model. Mater Struct 2009;42:301–20. https://doi.org/10.1617/s11527-008-9463-x.
[16] Källsner B, Girhammar UA. Plastic models for analysis of fully anchored light-frame timber shear walls. Eng Struct 2009;V31(I9):2171–81. https://doi.org/10.1016/j.engstruct.2009.03.023.
[17] Grossi P., Sartori T., Tomasi R. (2015). Tests on timber frame walls under in-plane forces: part 1. Proceedings of the Institution of Civil Engineers - Struct Build, 168 (11), 826–839. doi:10.1680/stbu.13.00107.
[18] Grossi P., Sartori T., Tomasi R. (2015). Tests on timber frame walls under in-plane forces: part 2. Proceedings of the Institution of Civil Engineers - Struct Build, 168 (11), 840–852. doi:10.1680/stbu.13.00108.
[19] Kramer L., Furrer L., Geiser M., Bemessung von Holzrahmenbau-Wänden mit Gipsfaserbeplankung, S-WIN Tagung, Biel/Bienne.
[20] Daniels HE. The statistical theory of the strength of bundles of threads. Proc R Soc Lond Ser A Math Phys Sci 1945;183(995):405–35. https://doi.org/10.1098/rspa.1945.0011.
[21] Gollwitzer S, Racewitz R. On the reliability of daniels systems. Struct Saf 1990;7: 229–43. https://doi.org/10.1016/0167-4730(90)90072-W.
[22] Beck AT, Da Silva LAR, Miguel LFF. The latent failure probability: a conceptual basis for robust, reliability-based and risk-based de-sign optimization. Reliab Eng Syst Saf 2023;233:109127. https://doi.org/10.1016/j.ress.2023.109127.
[23] Teichgräber M, Köhler J, Straub D. A generalized daniels system for reliability assessment of redundant structural systems redundancy effects in partial safety factor design: a link to a generalized daniels system. Technical University of Munich; 2023. ⟨https://www.cee.ed.tum.de/era/publications/⟩. visited Feb. 2024).
[24] Guers F, Dolinski K, Rackwitz R. Probability of failure of brittle redundant structural systems in time. Struct Saf 1988;5(3):169–85. https://doi.org/10.1016/0167-4730(88)90008-2.
[25] Guers F., Rackwitz R. (1987). Time-variant reliability of structural systems subject to fatigue. In: Proc. International Conference on Applications of Statistics and Probability in civil engineering (ICASP) 5.
[26] Schneider R, Thöns S, Rücker W, Straub D. Effect of different inspection strategies on the reliability of daniels systems subjected to fatigue. International Conference on Structural Safety and Reliability, 2013. ICOSSAR; 2013. 1637-264.
[27] International Organisation for Standardization ISO (2010) ISO 21581: Timber structures - Static and cyclic lateral load test methods for shear walls.
[28] European Committee for Standardization CEN (2005) EN 789: Timber structures - Test methods - Determination of mechanical properties of wood based panels.
[29] Manser N., in preparation, Entwicklung einer Methode für die Modellierung, Bemessung und Ausführung von aussteifenden Holzrahmenbau-Wänden mit Öffnungen, Dissertation, ETH Zürich.
[30] Ottenhaus LM, Jocker R, Drimmelen D, Crews K. Designing timber connections for ductility – a review and discussion. Con Build Mat 2021;v304. https://doi.org/10.1016/j.conbuildmat.2021.124621.
[31] Casagrande D., Polastri A., Sartori T., Loss C., Chiadega M., 2016, Experimental Campaign for the Mechanical Characterization of Connection Systems in the Seismic Design of Timber Buildings, World Conference on Timber Engineering (WCTE), Vienna Austria.
[32] Rossi S, Giongo I, Casagrande D, Tomasi R, Piazza M. 2019, evaluation of the displacement ductility for the seismic design of light-frame wood buildings. Bull Earthq Eng 2019;17:5313–38. https://doi.org/10.1007/s10518-019-00659-4.

[33] Geiser M, Bergmann M, Follesa M. Influence of steel properties on the ductility of doweled timber connections. Con Build Mat 2021;V266. https://doi.org/10.1016/j.conbuildmat.2020.121152.
[34] Geiser M, Furrer L, Kramer L, Blumer S, Follesa M. Investigations of connection detailing and steel properties for high ductility doweled timber connections. Con Build Mat 2022;V324. https://doi.org/10.1016/j.conbuildmat.2022.126670.
[35] Jockwer R, Caprio D, Jorissen A. Evaluation of parameters influencing the load-deformation behaviour of connections with laterally loaded dowel-type fasteners. N1 Wood Mat Sci Eng 2021;V17:6–9. https://doi.org/10.1080/17480272.2021.1955297.
[36] Jorissen A, Fragiacomo M. General notes on ductility in timber structures. I11 Eng Struct 2011;V33:2987–97. https://doi.org/10.1016/j.engstruct.2011.07.024.
[37] Leonard F, Mönnig E. Vorlesungen über massivbau - teil 1: grundlagen zur bemessung im stahlbetonbau. Heidelberg: Springer Berlin; 1984. https://doi.org/10.1007/978-3-642-61739-3.
[38] Leonard F, Mönnig E. Vorlesungen über massivbau - teil 2: Sonderfälle der bemessung im stahlbetonbau. Heidelberg: Springer Berlin; 1984. https://doi.org/10.1007/978-3-642-61643-3.
[39] Leonard F, Mönnig E. Vorlesungen über massivbau - teil 3: Grundlagen zum bewehren im stahlbetonbau. Heidelberg: Springer Berlin; 1984. https://doi.org/10.1007/978-3-642-61890-1.
[40] Dolan JD, Foschi RO. Structural analysis model for static loads on timber shear walls. J Struct Eng 1991;117(3):851–61. https://doi.org/10.1061/(ASCE)0733-9445(1991)117:3(851).
[41] JCSS Resistance Models Reinforcement Steel. JCSS Probabilistic Model Code, 2001, ⟨https://www.jcss-lc.org/publications/jcsspmc/rebar.pdf⟩, accessed 22.12.2023.
[42] JCSS Resistance Models Structural Steel. JCSS Probabilistic Model Code, 2001, ⟨https://www.jcss-lc.org/publications/jcsspmc/steelpr.pdf⟩, accessed 22.12.2023.
[43] JCSS Resistance Models Concrete. JCSS Probabilistic Model Code, 2002, ⟨https://www.jcss-lc.org/publications/jcsspmc/concrete.pdf⟩, accessed 22.12.2023.
[44] JCSS Resistance Models Timber. JCSS Probabilistic Model Code, 2006, ⟨https://www.jcss-lc.org/publications/jcsspmc/timber.pdf⟩, accessed 22.12.2023.
[45] Schilling S., 2022, Structural behaviour and reliability of timber trusses with dowelled steel-to-timber connections, Dissertation, ETH Zürich, https://doi.org/10.3929/ethz-b-000538109.
[46] Theiler M., 2014, Stabilität von Axial auf Druck beanspruchten Bauteilen aus Vollholz und Brettschichtholz, Dissertation, ETH Zürich, https://doi.org/10.3929/ethz-a-010273734.
[47] Schick M., 2017, Probabilistische Untersuchungen zu Überfestigkeiten von genagelten Wandelementen in Holztafelbauweise, Dissertation, Universität Kassel, doi:10.19211/KUP9783737602914.
[48] Melchers RE, Beck AT. Structural Reliability Analysis and Prediction. John Wiley & Sons Ltd; 2018. https://doi.org/10.1002/9781119266105.
[49] Huang C, El Hami A, Radi B. Overview of structural reliability analysis methods — part II: sampling methods. Incert Et fiabilité Des SystèMes multiphysiques 2017;17(1). https://doi.org/10.21494/iste.op.2017.0116.
[50] Virtanen P, Gommers R, Oliphant TE, Haberland M, Reddy T, Cournapeau D, et al. SciPy 1.0: fundamental algorithms for scientific computing in python. Nat Methods 2020;17(3):261–72. https://doi.org/10.1038/s41592-019-0686-2.
[51] European Committee for Standardization CEN (2002) EN 1990: Basis of structural design.
[52] McBean E., Rovers F.A., 1998, Statistical Procedures for Analysis of Environmental Monitoring Data & Risk Assessment, Prentice Hall PTR Environmental Management & Engineering Series, Volume 3, Prentice Hall, Upper Saddle River.
[53] Steel R.D., Torrie J.H., 1991, Prinsip dan Prosedur Statistika, Edition 2, Gramedia Pustaka Utama, JaBDKim3Sg-01.